X-ray imaging of the magnetic configuration of a three-dimensional artificial spin ice building block

Cite as: APL Mater. 10, 101101 (2022); doi: 10.1063/5.0101797
Submitted: 3 June 2022 • Accepted: 1 September 2022 •
Published Online: 4 October 2022

Petai Pip,[1,2,3,a)] Samuel Treves,[1,2,4,5] Jamie R. Massey,[1,2] Simone Finizio,[6] Zhaochu Luo,[1,2] Aleš Hrabec,[1,2] Valerio Scagnoli,[1,2] Jörg Raabe,[6] Laetitia Philippe,[3] Laura J. Heyderman,[1,2] and Claire Donnelly[7,8,b)]

AFFILIATIONS

[1] Laboratory for Mesoscopic Systems, Department of Materials, ETH Zurich, 8093 Zurich, Switzerland
[2] Laboratory for Multiscale Materials Experiments, Paul Scherrer Institute, PSI, 5232 Villigen, Switzerland
[3] EMPA (Swiss Federal Laboratories for Materials Testing and Research), 3602 Thun, Switzerland
[4] Department of Physics, University of Basel, 4056 Basel, Switzerland
[5] Swiss Nanoscience Institute, University of Basel, 4056 Basel, Switzerland
[6] Swiss Light Source, Paul Scherrer Institute, PSI, 5232 Villigen, Switzerland
[7] Max Planck Institute for Chemical Physics of Solids, Noethnitzer Str. 40, 01187 Dresden, Germany
[8] Cavendish Laboratory, University of Cambridge, JJ Thomson Ave., Cambridge CB3 0HT, United Kingdom

Note: This paper is part of the Special Topic on Science and Technology of 3D Magnetic Nanostructures.

[a)] **Electronic mail:** petai.pip@psi.ch
[b)] **Author to whom correspondence should be addressed:** claire.donnelly@cpfs.mpg.de

ABSTRACT

The extension of artificial spin systems to the third dimension offers advances in functionalities and opportunities for technological applications. One of the main challenges facing their realization is the fabrication of three-dimensional geometries with nanoscale resolution. In this work, we combine two-photon lithography with deformation-free pyrolysis and a GdCo coating to create a three-dimensional (3D) tripod structure that represents a building block of an 3D artificial spin ice, surrounded by a two-dimensional magnetic film. We map the three-dimensional magnetic configuration of the structure and its surroundings using soft x-ray magnetic laminography. In this way, we determine the magnetic configuration of the tripod nanostructure to be in the low-energy two-in-one-out spin ice state, observed at the 2D vertex of a kagome ice and predicted for three-dimensional vertices of magnetic buckyball structures. In contrast to isolated vertices, the degeneracy of this state can be lifted by the surrounding film, which also offers a route toward the controlled injection of emergent charges. This demonstration of the building block of a 3D spin system represents the first step toward the realization and understanding of more complex 3D artificial spin systems.

I. INTRODUCTION

Artificial spin ices,[1–3] consisting of arrays of dipolar-coupled nanomagnets, exhibit rich physics, including emergent magnetic monopoles[4] and phase transitions.[5–7] One of the main advantages of artificial spin systems is the possibility to create and tailor specific physical properties that comes with the freedom of design in contrast to bulk spin systems. Therefore, they have high potential for the realization of new applications, such as advanced computing devices,[8,9] nanomagnetic logic gates,[10,11] and programmable magnonic crystals.[12–14]

While most artificial spin systems are two-dimensional (2D), there is growing interest in the extension of such systems into the third dimension (3D), which offers additional degrees of

freedom and access to behaviors not realizable in planar systems.[15–17] Indeed, it has been shown that the limitations of non-equivalent interactions between nanomagnets at the vertices of a 2D square-lattice can be overcome by introducing a height displacement[18–20] so that signatures of the Coulomb phase can be observed.[21,22] In fact, experimental work on inverse opal-like structures[23–28] and gyroids[29] has highlighted that going toward three-dimensional (3D) artificial spin systems provides new environments to study frustration of magnetic systems, beyond the geometries restricted by 2D systems. However, self-assembly techniques, such as colloidal sphere lithography or block copolymer templating used for inverse opal-like and gyroid structures, respectively, do not offer exact tailoring of 3D geometries.

With the recent advance in 3D nanofabrication, the introduction of more complex 3D magnetic nanostructures is now possible. In this way, new topologies,[30,31] the introduction of chirality,[32–34] or designed frustrated lattices[35–37] are now possible, offering promising new directions for advanced applications. There are currently two routes for the fabrication of such complex magnetic nanostructures: first, the direct-writing of magnetic materials with focused electron beam induced deposition (FEBID). For FEBID, recent implementations of a computer aided design (CAD)-based model have opened the door to the fabrication of a wide variety of 3D architectures with typical nanowire diameters of tens of nanometers.[31,38–40] The second route concerns the deposition of magnetic materials on non-magnetic 3D scaffolds,[30,36,37,41,42] leading to the formation of 3D magnetic shell structures. These scaffolds can be realized either via FEBID[41] or via two-photon lithography,[36,42,43] a powerful technique capable of realizing arbitrary 3D geometries, though typically with larger scale features on the order of hundreds of nanometers. Recent progress in post-processing steps has led to the shrinking of structures to magnetically relevant lengthscales.[44] With deposition techniques, such as evaporation and sputtering, scaffolds can be magnetically coated with material properties with similar quality to thin films deposited on flat substrates.[41]

Here, we take advantage of these recent advances in nanofabrication to create a magnetic tripod nanostructure that represents a nanoscale building block of a frustrated 3D lattice. The building block consists of three legs, which can be approximated as Ising spins, meeting at a 3D vertex. This vertex is surrounded by a 2D magnetic film, providing a route to controlling the magnetic configuration. We use two-photon lithography to fabricate 3D polymeric microscaffolds. To achieve the lengthscales for which the magnetization is dominated by the 3D shape anisotropy, we perform pyrolysis on the scaffolds using deformation—preventing supports to homogeneously reduce their size by 70%, while retaining their 3D geometry. In a final step, we use DC magnetron sputtering to coat the sample with a magnetic GdCo layer to create a 3D shell structure. We note that with this technique, a homogeneous coating of the 3D structure is not possible and that shadowing effects[42] will lead to a half-tube-like magnetic shell.

The magnetic configuration of the frustrated structure is determined using soft x-ray magnetic laminography,[45,46] providing direct access to the 3D magnetization configuration. In contrast to previous studies, where magnetic force microscopy measurements indicated the presence of magnetic charges at the vertices, the use of x-ray imaging probes the magnetization itself. In this way, we are able to identify the specific configuration and, therefore, the "vertex type" present in the system. The use of laminography also provides access to buried layers within a 3D sample, offering a promising route to the study of extended lattices. Here, we observe that the magnetic configuration is determined by the geometrical frustration of the tripod nanostructure and the magnetization of the film in which the 3D structure is embedded. In particular, the tripod was found to be in a macroscopic low-energy 2-in-1-out spin ice state, similar to that observed in the two-dimensional analog vertex of a kagome lattice and found in 3D vertices of magnetic buckyball structures determined with micromagnetic simulations.[47]

Our approach provides a new platform to use building blocks such as the tripod to realize more complex lattices and study their intriguing physics, including charge propagation through 3D lattices, complex domain wall configurations, and the thermal relaxation of such systems toward the ground state. Moreover, the sensitivity of the x rays through the depth opens up the possibility to study lattices involving multiple layers.

II. SAMPLE FABRICATION

To create our tripod nanostructure, we first define a non-magnetic scaffold with two-photon lithography, which we subsequently coat with a magnetic material, as shown in Fig. 1. To achieve the lengthscales necessary for an artificial spin system, we combine two-photon lithography, which is ideal for the definition of micrometer-sized structures, with pyrolysis, a procedure that involves the thermal decomposition of a material by a high temperature treatment in an inert gas atmosphere. This treatment leads to significant shrinking of the structure and the conversion from a polymer to a glassy carbon, which is ideal for the prevention of x-ray dose-induced deformations or damage.[42] One challenge associated with pyrolysis involves deformations of the structure during the shrinking process as the part of the structure attached to the substrate will retain its pre-pyrolysis dimensions. To ensure the homogeneous shrinkage of the geometry, we fabricate the tripod structure on a hemi-spherical support, which we have found is a robust technique to maintain complex 3D geometries during resizing, as shown schematically in Fig. 1(b). The homogeneous shrinking of the structure provides a key advantage of this combined process, allowing one to overcome the elongated cross section of wires typically obtained with high resolution two photon lithography and pattern truly arbitrary geometries with a high degree of accuracy.

Specifically, the 3D polymeric microscaffold fabricated with two-photon lithography [see Fig. 1(a)] consists of a tripod structure with 60° inclined branches with angles between the nanowires of 120°, a cylindrical diameter of 800 nm, and a length of 8 μm, centered on a hemisphere shaped support with a diameter of 15 μm. To ensure compatibility with x-ray microscopy measurements, the structure is fabricated on an x-ray transparent silicon nitride membrane. In order to shrink the tripod to the nanoscale, the polymeric scaffold was pyrolyzed by heating the sample to 690 °C in a nitrogen atmosphere for 5.2 h, leading to a reduction in size of 70%. In particular, the diameter of the half-sphere reduces to 4 μm, while the tripod branches were reduced to a length and diameter of 880 and 160 nm, respectively, maintaining the 60° inclination.

In a final step, the pyrolyzed scaffold was coated with 30 nm of GdCo using DC magnetron sputtering that offers the deposition of a

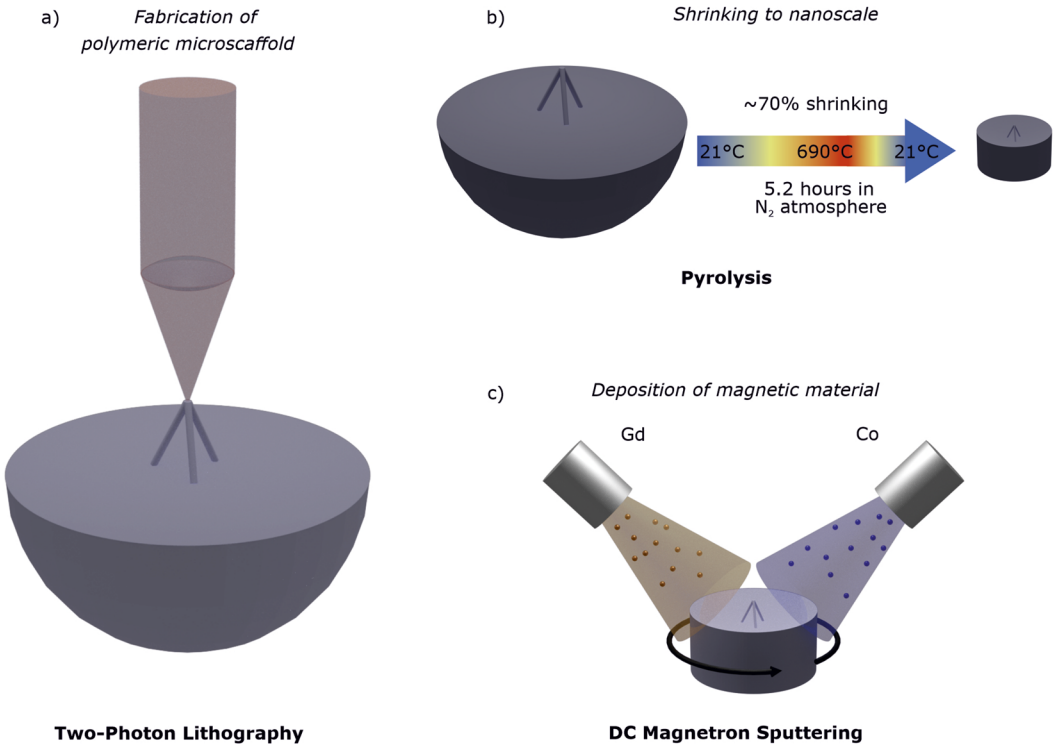

FIG. 1. Sample fabrication in three steps: (a) Fabrication of a polymeric microscaffold on a hemisphere support with two-photon lithography. (b) Pyrolysis of the polymeric microscaffold, resulting in ~70 % shrinkage. (c) Coating of a magnetic GdCo layer with DC magnetron sputtering.

high-quality amorphous magnetic material with high x-ray magnetic circular dichroism (XMCD) contrast and low magnetocrystalline anisotropy. During the deposition, the stage is rotated to improve the homogeneity of the film and give a uniform deposition, as shown in Fig. 1(c). Due to the non-local nature of the deposition, the material is deposited both on the tripod structure and on the surface of the support pillar, providing an interface between the 2D film and the 3D nanostructure.

III. IMAGING OF THREE-DIMENSIONAL MAGNETIC CONFIGURATION

Having fabricated our 3D magnetic nanostructure, we next consider its as-grown 3D magnetic configuration and the influence of the non-trivial 3D geometry. Traditional techniques used for the characterization of artificial spin systems have involved the use of surface-sensitive techniques, such as x-ray photoelectron emission microscopy (X-PEEM), which provides access to the surface magnetization, or magnetic force microscopy (MFM), which offers surface sensitivity to local charges in the magnetization. For 3D artificial spin systems, however, we require a high spatial resolution depth-sensitive probe of the magnetization state. For this, we turn to 3D x-ray magnetic imaging techniques, which offer a nanoscale mapping of the 3D magnetization through the thickness of a system.[45,46,48,49] First developed for the tomographic geometry, 3D x-ray magnetic imaging has led to the observation of magnetic features within the bulk, such as Bloch point singularities[48,49] and magnetic vortex rings.[50] The extension to the laminography geometry,[45,46] where the rotation axis is no longer perpendicular to the x-ray beam, has made possible the study of the statics and dynamics of extended samples,[45,46,51] opening the door to the study of lithographically patterned structures mounted on x-ray transparent membranes, such as our current system. Here, we exploit soft x-ray magnetic laminography to map the static three-dimensional magnetic configuration of the tripod nanostructure.

A. X-ray magnetic laminography

Synchrotron x-ray magnetic laminography involves the measurement of 2D projections of the magnetization for different sample orientations about a rotation axis. As shown schematically in Fig. 2(a), the laminography rotation axis is oriented at 45° to the x-ray beam. Sensitivity to the magnetization is obtained by exploiting x-ray magnetic circular dichroism (XMCD). Specifically, the energy of the x rays is tuned to the L_3 absorption edge of Cobalt, and scanning transmission x-ray microscopy (STXM) images are measured with circular left and right polarized x rays, providing access to the projection of the magnetization parallel to the direction of the x-ray beam[46,52] (see the supplementary material).

XMCD projections of the magnetic tripod nanostructure oriented at angles of 0°, 96°, 180°, and 272° about the rotation axis

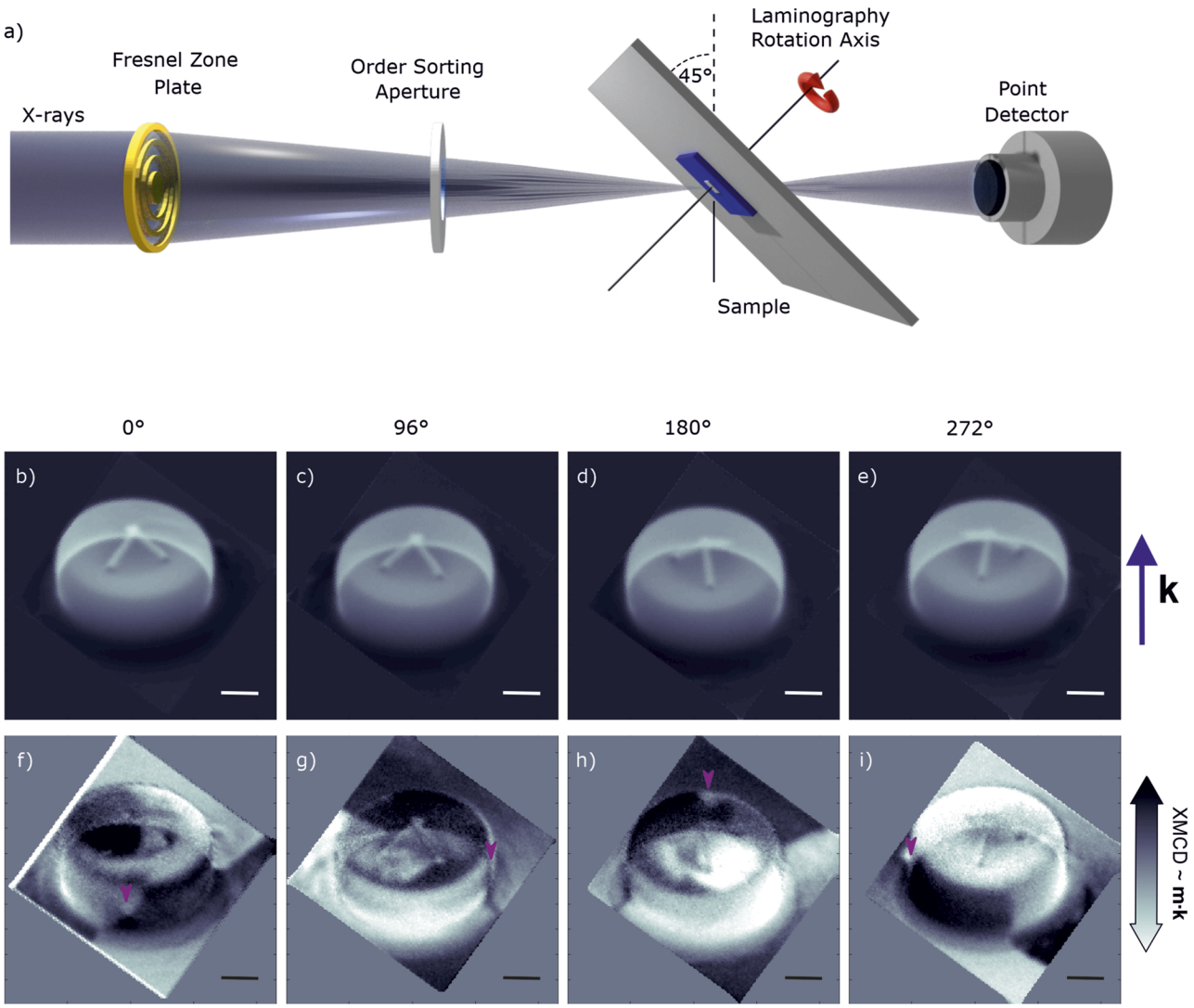

FIG. 2. (a) Soft x-ray laminography setup with the rotation axis tilted at 45° to the x-ray beam. The samples are scanned by a nanofocused x-ray beam, detected in transmission using a photodiode. The sample stage is rotated around its normal (laminography rotation axis). 2D projections of the electronic contrast (b)–(e) and the magnetization (f)–(i) of the magnetic tripod nanostructure on a micropillar at different sample rotation angles. (b)–(e) In the projections of the electronic contrast, as the angle is changed from (b) to (e), the projection of the symmetric pillar is constant, while the tripod can be seen to rotate. (f)–(i) In the 2D projections of the XMCD contrast (double-headed arrow) that indicates the direction of the magnetization parallel to the direction of the x rays (indicated by the blue arrow), significant changes in the contrast with angle can be observed. The purple arrow tracks a domain wall in the side of the pillar, thus indicating the direction of rotation of the sample. Scale bars represent 1 μm.

are given in Figs. 2(b)–2(e), where bright and dark regions correspond to the magnetization pointing parallel and antiparallel to the x-ray beam, respectively. As can be seen in the projections, the XMCD signal is not limited to the tripod structure, but is a combination of signals from the planar film background, the micropillar, and the 3D nanostructure, confirming the fact that the 3D nanostructure is surrounded by a continuous film, as expected from the deposition.

We can first obtain an indication of the magnetic structure by considering the 2D XMCD projections in Figs. 2(b)–2(e). We note that the x rays are incident along the plane parallel to the vertical axis of the image, indicated by the blue arrow (**k**), meaning that the bright and dark regions correspond to the magnetization aligning parallel and antiparallel to this direction. The laminography angle is 45°, meaning that both the in-plane and out-of-plane components of the magnetisation are probed. We first note a structure in the

magnetization in the side wall of the support pillar [indicated by the purple arrow in Figs. 2(b)–2(e)] that corresponds to the presence of a change in the direction of the magnetization and a domain wall. As we rotate the sample, we observe that the domain wall rotates until at 180°, the structure is found on the other side. Interestingly, we can see that the contrast of the domains does not change as the sample is rotated, indicating that the magnetization is aligned parallel to the rotation axis. Second, we also observe magnetic domain structures in the flat plane on the top of the support pillar that, after a rotation of 180°, change contrast, indicating that they are oriented perpendicular to the rotation axis, in the plane of the sample.

While a first indication of the magnetic configuration can be obtained by comparing 2D projections at different angles, to determine the exact 3D magnetic configuration, we perform magnetic laminography. Specifically, we measure 94 XMCD projections equally spaced about 360°. The 3D magnetization configuration is, then, reconstructed using a graphics processing unit (GPU) implementation of the gradient-based optimization routine presented in Ref. 52.

B. Reconstruction of the 3D magnetic vector field

The reconstruction of the 3D magnetic vector field is shown in Fig. 3(a) where one can see the configuration of all three parts of the structure: the sides and top surface of the support pillar and the magnetic tripod itself. Two further views of the reconstruction at different orientations are given in the supplementary material in Fig. 1.

We start by considering the larger magnetic structure of the support pillar surface in which the ends of the tripod legs are embedded. In agreement with our interpretation of the 2D projections of the structure, we observe that the magnetization on the sides of the pillar is generally aligned in the plane of the film, parallel to the rotation axis, and forms domains of opposite directions of the magnetization, indicating the presence of uniaxial anisotropy. This is in contrast to the top surface of the pillar, where the magnetization lies in the plane, but does not display a preferred orientation. This difference in the orientation of the magnetization can be understood by considering the deposition of the material: the GdCo film is deposited at an angle of 45° to the substrate, and the sample is rotated about its normal during the deposition. For a material deposited at a constant oblique angle to a surface, an in-plane anisotropy parallel to the direction of deposition is known to occur.[53] For the top surface, the continuous in-plane rotation during deposition removes this anisotropy. However, on the vertical sides of the pillar, shadowing effects mean that a vertical uniaxial anisotropy is induced, resulting in the observed domains.

In contrast to the well-defined domains that form on the vertical sides of the support pillar, on the top surface, a more twisted magnetic configuration is observed, which appears to relate to the magnetic configuration of the tripod. Indeed, when considering the magnetic structure of the tripod in Figs. 3(b) and 3(c), one can see that the magnetic moments in each of the branches are aligned with the shape geometry, forming a macroscopic moment along the longitudinal axes [Figs. 3(d) and 3(e)]. These uniaxial orientations demonstrate the successful realization of macroscopic Ising spins in the building block of a 3D artificial spin system.

The tripod is in effect a 3D vertex with three branches and, therefore, an effective extension of the in-plane frustrated kagome spin ice[4,54] into the third dimension. Indeed, the system represents a step between the in-plane kagome system and the out-of-plane kagome[55] or triangular[56] Ising spin lattices and, thus, represents an opportunity to explore the phase space between the two systems.

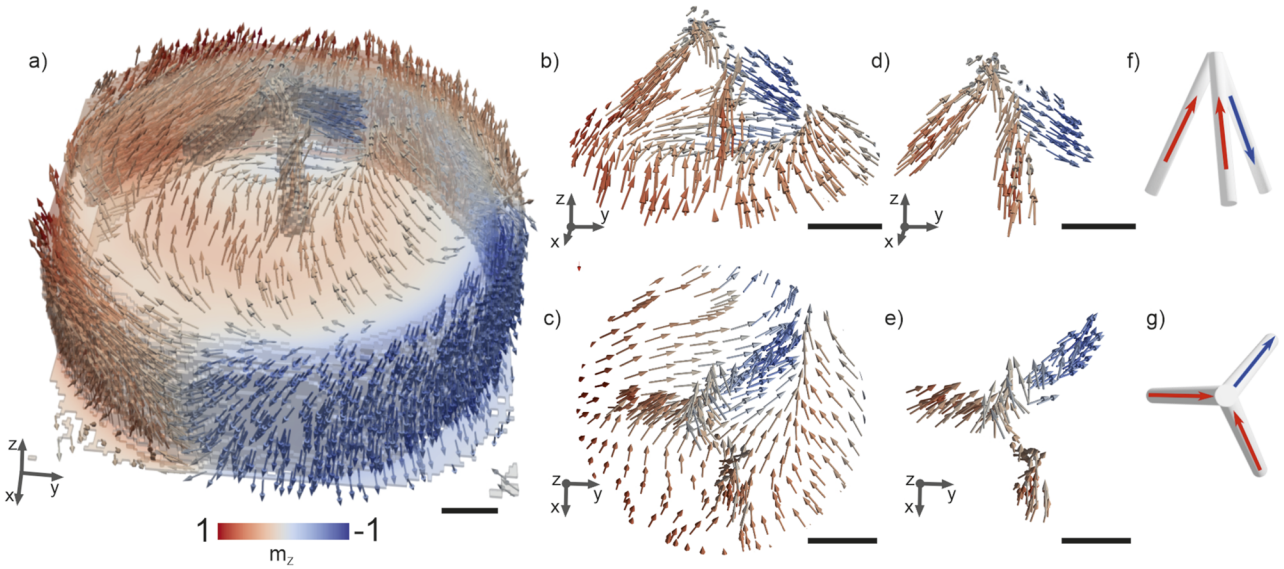

FIG. 3. Reconstruction of the 3D magnetic vector field of the tripod nanostructure on a support pillar. (a) The overall reconstructed configuration of the sample, showing the $\hat{z}$ orientation of the side walls, and the in-plane magnetization of the top surface of the support pillar. The configuration of the tripod is shown in (b)–(e), where one can see from the side (b) and (d) and top (c) and (e) views that the tripod forms a two-in one-out Ising spin state, shown schematically in (f) and (g). Scale bars represent 500 nm.

Similar to the magnetic configurations of the vertices of the 2D kagome ice, we expect there to be six degenerate ground states of the isolated vertex, which consist of the different combinations of two macroscopic moments pointing into or out of the vertex and the third one being reversed. In addition, higher energy states are formed when all three macroscopic moments point into or out of the vertex.

Here, while in two branches, the macroscopic moment is pointing upward toward the center of the vertex, the spin of the third branch is reversed. This two-in, one-out magnetic configuration is, indeed, analogous to a lowest energy spin ice configuration of a vertex in the 2D artificial kagome spin ice. In addition, this magnetic configuration has been observed in micromagnetic simulations of buckyball structures, consisting of 3D vertices with three branches.[47]

We note that there is a link between the magnetic configuration in the tripod and that of the 2D thin film to which it is connected. Here, we observe, in the as-grown magnetic state, that the magnetization on the top surface of the pillar forms a twisted state that follows the magnetic moments of the tripod branches. This promotes the smooth transition between the magnetization in the 2D film and the 3D structure and, therefore, a lower energy state. In particular, the interface between the 2D film and the 3D structure could be exploited to lift the degeneracy of the two-in (out), one-out (in) states.

With the reconstruction of the 3D magnetic vector field of the sample, we are able to map out the magnetic configuration of both the 3D nanostructure and its surroundings, providing insights into the interplay between the tripod and the surface of the pillar. This direct access to the 3D magnetic configuration is immediately extendable to thicker systems, opening up the study of artificial spin systems made up of several layers, which is not possible with surface-sensitive characterization methods, such as MFM. Furthermore, the observation of the interplay between the magnetic configuration in the 2D film and the 3D structure opens up new routes to control 3D artificial spin systems by lifting the degeneracy of frustrated spin states with the magnetic underlayers. Analogous to the use of nanomagnets with different switching fields for nanomagnetic logic[10] and the introduction of a switchable underlayer in 2D artificial spin systems,[57] the 2D magnetic film could be exploited to control the magnetic state of the 3D vertex. In addition, by switching its magnetization with an external magnetic field or current, the film could act as an injection pad for domain walls,[41] offering a route to the controllable injection of emergent magnetic charges into the spin system.

IV. CONCLUSIONS AND OUTLOOK

In this work, we have realized a nanoscale building block of a three-dimensional artificial spin system on top of a planar magnetic film. By determining the magnetic configuration of the tripod structure and its surroundings with soft x-ray magnetic laminography, we find that each of the three nanoscale branches are single domain and, thus, represent a macroscopic Ising-like spin. A low energy spin ice state was observed in which the magnetic moments of two tripod branches are pointing into the 3D vertex, while the moment is reversed in the third branch. Moreover, in contrast to isolated systems with multiple degenerate vertex states, here, the magnetic configuration is determined by both the 3D geometry and the interface with the magnetization of the underlying 2D film. Indeed, this 2D film can be exploited to lift the degeneracy of the vertex states and be used for the controlled injection of magnetic charges into a 3D artificial spin system.

The nanoscale three-dimensional vertex structure was achieved via a combination of two photon lithography and pyrolysis. Key to the realization of the 3D geometry with nanoscale resolution was the development of a support structure, which ensured the homogeneous shrinkage of the 3D geometry during pyrolysis. This route to achieving 3D geometries with nanoscale dimensions and arbitrary geometries opens the door to the realization of robust 3D scaffolds with feature sizes significantly smaller than those achievable with standard two-photon lithography. In such a vertex nanostructure, the control over the 3D geometry allows for the frustration of the building block to be tuned by the variation of the inter-nanotube angles. Moreover, the technique offers the possibility of implementing a large variety of geometries and shapes. For example, combining multiple building blocks could lead to the realization of designed, complex 3D lattices, opening the door to the experimental study of phenomena, such as charge propagation in 3D that could be revealed by tracking the three-dimensional configuration under the application of magnetic fields. Understanding such complex three-dimensional magnetic systems necessitates a step-by-step approach, and the enhanced understanding of the magnetic behavior of three-dimensional building blocks is an important step toward the elucidation of the behavior of truly three-dimensional artificial spin systems.

SUPPLEMENTARY MATERIAL

See the supplementary material for further details of the sample fabrication and the x-ray laminography measurement.

ACKNOWLEDGMENTS

Petai Pip and Laura J. Heyderman acknowledge funding from the Swiss National Science Foundation (Project No. 200020_172774). Claire Donnelly acknowledges funding from the Leverhulme Trust (Grant No. ECF-2018-016), the Isaac Newton Trust (Grant No. 18-08), the L'Oréal–UNESCO UK and Ireland Fellowship For Women In Science 2019, and the Max Planck Society Lise Meitner Excellence Program. Part of this work was performed at the PolLux (Grant No. X07DA) beamline of the Swiss Light Source, Paul Scherrer Institute, Villigen PSI, Switzerland. The PolLux endstation was financed by the German Bundesministerium für Bildung und Forschung (BMBF) through Contract Nos. 05K16WED and 05K19WE2. Sam Treves and Valerio Scagnoli acknowledge support from the Swiss Nanoscience Institute at the University of Basel. Jamie Massey and Valerio Scagnoli acknowledge funding from the Swiss National Science Foundation (Project No. SNF 200021_192162).

AUTHOR DECLARATIONS

Conflict of Interest

The authors have no conflicts to disclose.

Author Contributions

Petai Pip: Conceptualization (equal); Data curation (equal); Formal analysis (equal); Methodology (equal); Writing – original draft (equal); Writing – review & editing (equal). **Samuel Treves**: Data curation (equal); Formal analysis (equal); Methodology (equal); Writing - original draft (equal). **Jamie Massey**: Data curation (equal); Methodology (equal); Writing – review & editing (equal). **Simone Finizio**: Data curation (equal); Methodology (equal). **Zhaochu Luo**: Methodology (equal). **Aleš Hrabec**: Methodology (equal). **Valerio Scagnoli**: Methodology (equal). **Jörg Raabe**: Methodology (equal). **Laetitia Philippe**: Conceptualization (equal); Funding acquisition (equal); Project administration (equal); Resources (equal); Supervision (equal). **Laura J. Heyderman**: Conceptualization (equal); Funding acquisition (equal); Project administration (equal); Resources (equal); Supervision (equal). **Claire Donnelly**: Conceptualization (equal); Data curation (equal); Formal analysis (equal); Methodology (equal); Supervision (equal); Visualization (equal).

DATA AVAILABILITY

The data associated with this manuscript is available at 10.5281/zenodo.7108141. A version of the analysis codes are found at 10.5281/zenodo.1324335.

REFERENCES

[1] L. J. Heyderman and R. L. Stamps, "Artificial ferroic systems: Novel functionality from structure, interactions and dynamics," J. Phys.: Condens. Matter **25**, 363201 (2013).

[2] C. Nisoli, R. Moessner, and P. Schiffer, "Colloquium: Artificial spin ice: Designing and imaging magnetic frustration," Rev. Mod. Phys. **85**, 1473–1490 (2013).

[3] S. H. Skjærvø, C. H. Marrows, R. L. Stamps, and L. J. Heyderman, "Advances in artificial spin ice," Nat. Rev. Phys. **2**, 13 (2020).

[4] E. Mengotti, L. J. Heyderman, A. F. Rodríguez, F. Nolting, R. V. Hügli, and H.-B. Braun, "Real-space observation of emergent magnetic monopoles and associated Dirac strings in artificial kagome spin ice," Nat. Phys. **7**, 68 (2011).

[5] V. Kapaklis, U. B. Arnalds, A. Harman-Clarke, E. T. Papaioannou, M. Karimipour, P. Korelis, A. Taroni, P. C. W. Holdsworth, S. T. Bramwell, and B. Hjörvarsson, "Melting artificial spin ice," New J. Phys. **14**, 035009 (2012).

[6] L. Anghinolfi, H. Luetkens, J. Perron, M. G. Flokstra, O. Sendetskyi, A. Suter, T. Prokscha, P. M. Derlet, S. L. Lee, and L. J. Heyderman, "Thermodynamic phase transitions in a frustrated magnetic metamaterial," Nat. Commun. **6**, 8278 (2015).

[7] O. Sendetskyi, V. Scagnoli, N. Leo, L. Anghinolfi, A. Alberca, J. Lüning, U. Staub, P. M. Derlet, and L. J. Heyderman, "Continuous magnetic phase transition in artificial square ice," Phys. Rev. B **99**, 214430 (2019).

[8] J. H. Jensen, E. Folven, and G. Tufte, "Computation in artificial spin ice," *The 2018 Conference on Artificial Life* (ALIFE, 2018), pp. 15–22.

[9] J. H. Jensen and G. Tufte, "Reservoir computing in artificial spin ice," *The 2020 Conference on Artificial Life* (ALIFE, 2020), pp. 376–383.

[10] H. Arava, P. M. Derlet, J. Vijayakumar, J. Cui, N. S. Bingham, A. Kleibert, and L. J. Heyderman, "Computational logic with square rings of nanomagnets," Nanotechnology **29**, 265205 (2018).

[11] H. Arava, N. Leo, D. Schildknecht, J. Cui, J. Vijayakumar, P. M. Derlet, A. Kleibert, and L. J. Heyderman, "Engineering relaxation pathways in building blocks of artificial spin ice for computation," Phys. Rev. Appl. **11**, 054086 (2019).

[12] M. Krawczyk and D. Grundler, "Review and prospects of magnonic crystals and devices with reprogrammable band structure," J. Phys.: Condens. Matter **26**, 123202 (2014).

[13] S. Gliga, E. Iacocca, and O. G. Heinonen, "Dynamics of reconfigurable artificial spin ice: Toward magnonic functional materials," APL Mater. **8**, 040911 (2020).

[14] M. T. Kaffash, S. Lendinez, and M. B. Jungfleisch, "Nanomagnonics with artificial spin ice," Phys. Lett. A **402**, 127364 (2021).

[15] R. Streubel, P. Fischer, F. Kronast, V. P. Kravchuk, D. D. Sheka, Y. Gaididei, O. G. Schmidt, and D. Makarov, "Magnetism in curved geometries," J. Phys. D: Appl. Phys. **49**, 363001 (2016).

[16] A. Fernández-Pacheco, R. Streubel, O. Fruchart, R. Hertel, P. Fischer, and R. P. Cowburn, "Three-dimensional nanomagnetism," Nat. Commun. **8**, 15756 (2017).

[17] D. D. Sheka, "A perspective on curvilinear magnetism," Appl. Phys. Lett. **118**, 230502 (2021).

[18] G.-W. Chern, C. Reichhardt, and C. Nisoli, "Realizing three-dimensional artificial spin ice by stacking planar nano-arrays," Appl. Phys. Lett. **104**, 013101 (2014).

[19] G. Möller and R. Moessner, "Artificial square ice and related dipolar nanoarrays," Phys. Rev. Lett. **96**, 237202 (2006).

[20] L. A. S. Mól, W. A. Moura-Melo, and A. R. Pereira, "Conditions for free magnetic monopoles in nanoscale square arrays of dipolar spin ice," Phys. Rev. B **82**, 054434 (2010).

[21] Y. Perrin, B. Canals, and N. Rougemaille, "Extensive degeneracy, Coulomb phase and magnetic monopoles in artificial square ice," Nature **540**, 410 (2016).

[22] A. Farhan, M. Saccone, C. F. Petersen, S. Dhuey, R. V. Chopdekar, Y. L. Huang, N. Kent, Z. Chen, M. J. Alava, T. Lippert, A. Scholl, and S. van Dijken, "Emergent magnetic monopole dynamics in macroscopically degenerate artificial spin ice," Sci. Adv. **5**, eaav6380 (2019).

[23] S. V. Grigoriev, K. S. Napolskii, N. A. Grigoryeva, A. V. Vasilieva, A. A. Mistonov, D. Y. Chernyshov, A. V. Petukhov, D. V. Belov, A. A. Eliseev, A. V. Lukashin, Y. D. Tretyakov, A. S. Sinitskii, and H. Eckerlebe, "Structural and magnetic properties of inverse opal photonic crystals studied by x-ray diffraction, scanning electron microscopy, and small-angle neutron scattering," Phys. Rev. B **79**, 045123 (2009).

[24] N. A. Grigoryeva, A. A. Mistonov, K. S. Napolskii, N. A. Sapoletova, A. A. Eliseev, W. Bouwman, D. V. Byelov, A. V. Petukhov, D. Y. Chernyshov, H. Eckerlebe, A. V. Vasilieva, and S. V. Grigoriev, "Magnetic topology of Co-based inverse opal-like structures," Phys. Rev. B **84**, 064405 (2011).

[25] I. S. Shishkin, A. A. Mistonov, I. S. Dubitskiy, N. A. Grigoryeva, D. Menzel, and S. V. Grigoriev, "Nonlinear geometric scaling of coercivity in a three-dimensional nanoscale analog of spin ice," Phys. Rev. B **94**, 064424 (2016).

[26] A. A. Mistonov, N. A. Grigoryeva, A. V. Chumakova, H. Eckerlebe, N. A. Sapoletova, K. S. Napolskii, A. A. Eliseev, D. Menzel, and S. V. Grigoriev, "Three-dimensional artificial spin ice in nanostructured Co on an inverse opal-like lattice," Phys. Rev. B **87**, 220408 (2013).

[27] I. S. Dubitskiy, A. A. Mistonov, N. A. Grigoryeva, and S. V. Grigoriev, "Dependence of the inverse opal magnetic form-factor on the degree of sintering: Micromagnetic study," Physica B **549**, 107 (2017).

[28] A. Mistonov, I. Dubitskiy, I. Shishkin, N. Grigoryeva, A. Heinemann, N. A. Sapoletova, G. Valkovskiy, and S. V. Grigoriev, "Magnetic structure of the promising candidate for three-dimensional artificial spin ice: small angle neutron diffraction and micromagnetic simulations," J. Magn. Magn. Mater. **477**, 99 (2019).

[29] J. Llandro, D. M. Love, A. Kovács, J. Caron, K. N. Vyas, A. Kákay, R. Salikhov, K. Lenz, J. Fassbender, M. R. J. Scherer, C. Cimorra, U. Steiner, C. H. W. Barnes, R. E. Dunin-Borkowski, S. Fukami, and H. Ohno, "Visualizing magnetic structure in 3D nanoscale Ni–Fe gyroid networks," Nano Lett. **20**, 3642–3650 (2020).

[30] P. Pip, C. Donnelly, M. Döbeli, C. Gunderson, L. J. Heyderman, and L. Philippe, "Electroless deposition of Ni–Fe alloys on scaffolds for 3D nanomagnetism," Small **16**, 2004099 (2021).

[31] L. Skoric, D. Sanz-Hernández, F. Meng, C. Donnelly, S. Merino-Aceituno, and A. Fernández-Pacheco, "Layer-by-layer growth of complex-shaped three-dimensional nanostructures with focused electron beams," Nano Lett. **20**, 184–191 (2020).

[32] X. Li, H. Zhao, C. Liu, J. Cai, Y. Zhang, Y. Jiang, and D. Zhang, "High-efficiency alignment of 3D biotemplated helices via rotating magnetic field for terahertz chiral metamaterials," Adv. Opt. Mater. **7**, 1900247 (2019).

[33]D. Sanz-Hernández, A. Hierro-Rodriguez, C. Donnelly, J. Pablo-Navarro, A. Sorrentino, E. Pereiro, C. Magén, S. McVitie, J. M. De Teresa, S. Ferrer, P. Fischer, and A. Fernández-Pacheco, "Artificial double-helix for geometrical control of magnetic chirality," ACS Nano **14**, 8084 (2020).
[34]C. Donnelly, A. Hierro-Rodríguez, C. Abert, K. Witte, L. Skoric, D. Sanz-Hernández, S. Finizio, F. Meng, S. McVitie, J. Raabe, D. Suess, R. Cowburn, and A. Fernández-Pacheco, "Complex free-space magnetic field textures induced by three-dimensional magnetic nanostructures," Nat. Nanotechnol. **17**, 136–142 (2022).
[35]S. Sahoo, A. May, A. van Den Berg, A. K. Mondal, S. Ladak, and A. Barman, "Observation of coherent spin waves in a three-dimensional artificial spin ice structure," Nano Lett. **21**, 4629–4635 (2021).
[36]A. May, M. Hunt, A. Van Den Berg, A. Hejazi, and S. Ladak, "Realisation of a frustrated 3D magnetic nanowire lattice," Commun. Phys. **2**, 13 (2019).
[37]A. May, M. Saccone, A. van den Berg, J. Askey, M. Hunt, and S. Ladak, "Magnetic charge propagation upon a 3D artificial spin-ice," Nat. Commun. **12**, 3217 (2021).
[38]A. Fernández-Pacheco, L. Serrano-Ramón, J. M. Michalik, M. R. Ibarra, J. M. De Teresa, L. O'Brien, D. Petit, J. Lee, and R. P. Cowburn, "Three dimensional magnetic nanowires grown by focused electron-beam induced deposition," Sci. Rep. **3**, 1492 (2013).
[39]J. M. De Teresa, A. Fernández-Pacheco, R. Córdoba, L. Serrano-Ramón, S. Sangiao, and M. R. Ibarra, "Review of magnetic nanostructures grown by focused electron beam induced deposition (FEBID)," J. Phys. D: Appl. Phys. **49**, 243003 (2016).
[40]L. Keller, M. K. I. Al Mamoori, J. Pieper, C. Gspan, I. Stockem, C. Schröder, S. Barth, R. Winkler, H. Plank, M. Pohlit, J. Müller, and M. Huth, "Direct-write of free-form building blocks for artificial magnetic 3D lattices," Sci. Rep. **8**, 6160 (2018).
[41]D. Sanz-Hernández, R. F. Hamans, J.-W. Liao, A. Welbourne, R. Lavrijsen, and A. Fernández-Pacheco, "Fabrication, detection, and operation of a three-dimensional nanomagnetic conduit," ACS Nano **11**, 11066–11073 (2017).
[42]C. Donnelly, M. Guizar-Sicairos, V. Scagnoli, M. Holler, T. Huthwelker, A. Menzel, I. Vartiainen, E. Müller, E. Kirk, S. Gliga, J. Raabe, and L. J. Heyderman, "Element-specific x-ray phase tomography of 3D structures at the nanoscale," Phys. Rev. Lett. **114**, 115501 (2015).
[43]G. Williams, M. Hunt, B. Boehm, A. May, M. Taverne, D. Ho, S. Giblin, D. Read, J. Rarity, R. Allenspach, and S. Ladak, "Two-photon lithography for 3D magnetic nanostructure fabrication," Nano Res. **11**, 845–854 (2018).
[44]G. Seniutinas, A. Weber, C. Padeste, I. Sakellari, M. Farsari, and C. David, "Beyond 100 nm resolution in 3D laser lithography—Post processing solutions," Microelectron. Eng. **191**, 25–31 (2018).
[45]C. Donnelly, S. Finizio, S. Gliga, M. Holler, A. Hrabec, M. Odstrčil, S. Mayr, V. Scagnoli, L. J. Heyderman, M. Guizar-Sicairos, and J. Raabe, "Time-resolved imaging of three-dimensional nanoscale magnetization dynamics," Nat. Nanotechnol. **15**, 356–360 (2020).
[46]K. Witte, A. Späth, S. Finizio, C. Donnelly, B. Watts, B. Sarafimov, M. Odstrcil, M. Guizar-Sicairos, M. Holler, R. H. Fink, and J. Raabe, "From 2D STXM to 3D imaging: Soft x-ray laminography of thin specimens," Nano Lett. **20**, 1305–1314 (2020).
[47]R. Cheenikundil and R. Hertel, "Switchable magnetic frustration in buckyball nanoarchitectures," Appl. Phys. Lett. **118**, 212403 (2021).
[48]C. Donnelly, M. Guizar-Sicairos, V. Scagnoli, S. Gliga, M. Holler, J. Raabe, and L. J. Heyderman, "Three-dimensional magnetization structures revealed with X-ray vector nanotomography," Nature **547**, 328 (2017).
[49]A. Hierro-Rodriguez, C. Quirós, A. Sorrentino, L. M. Alvarez-Prado, J. I. Martín, J. M. Alameda, S. McVitie, E. Pereiro, M. Vélez, and S. Ferrer, "Revealing 3D magnetization of thin films with soft X-ray tomography: Magnetic singularities and topological charges," Nat. Commun. **11**, 6382 (2020).
[50]C. Donnelly, K. L. Metlov, V. Scagnoli, M. Guizar-Sicairos, M. Holler, N. S. Bingham, J. Raabe, L. J. Heyderman, N. R. Cooper, and S. Gliga, "Experimental observation of vortex rings in a bulk magnet," Nat. Phys. **17**, 316 (2021).
[51]S. Finizio, C. Donnelly, S. Mayr, A. Hrabec, and J. Raabe, "Three-dimensional vortex gyration dynamics unraveled by time-resolved soft x-ray laminography with freely selectable excitation frequencies," Nano Lett. **22**, 1971 (2022).
[52]C. Donnelly, S. Gliga, V. Scagnoli, M. Holler, J. Raabe, L. J. Heyderman, and M. Guizar-Sicairos, "Tomographic reconstruction of a three-dimensional magnetization vector field," New J. Phys. **20**, 083009 (2018).
[53]D. O. Smith, M. S. Cohen, and G. P. Weiss, "Oblique incidence anisotropy in evaporated permalloy films," J. Appl. Phys. **31**, 1755–1762 (1960).
[54]E. Mengotti, L. J. Heyderman, A. Fraile Rodríguez, A. Bisig, L. Le Guyader, F. Nolting, and H. B. Braun, "Building blocks of an artificial kagome spin ice: Photoemission electron microscopy of arrays of ferromagnetic islands," Phys. Rev. B **78**, 144402 (2008).
[55]S. Zhang, J. Li, I. Gilbert, J. Bartell, M. J. Erickson, Y. Pan, P. E. Lammert, C. Nisoli, K. K. Kohli, R. Misra, V. H. Crespi, N. Samarth, C. Leighton, and P. Schiffer, "Perpendicular magnetization and generic realization of the Ising model in artificial spin ice," Phys. Rev. Lett. **109**, 087201 (2012).
[56]E. Mengotti, L. J. Heyderman, A. Bisig, A. Fraile Rodríguez, L. Le Guyader, F. Nolting, and H. B. Braun, "Dipolar energy states in clusters of perpendicular magnetic nanoislands," J. Appl. Phys. **105**, 113113 (2009).
[57]S. Kempinger, Y.-S. Huang, P. Lammert, M. Vogel, A. Hoffmann, V. H. Crespi, P. Schiffer, and N. Samarth, "Field-tunable interactions and frustration in underlayer-mediated artificial spin ice," Phys. Rev. Lett. **127**, 117203 (2021).